Kinetic proofreading can explain the supression of supercoiling of circular DNA molecules by type-II topoisomerases

Jie Yan,[1] Marcelo O. Magnasco,[2] and John F. Marko[1]
[1]*Department of Physics, The University of Illinois at Chicago, 845 West Taylor Street, Chicago, Illinois 60607*
[2]*Center for Studies in Physics and Biology, The Rockefeller University, 1230 York Avenue, New York, New York 10021*
(Received 28 April 2000; revised manuscript received 22 August 2000; published 27 February 2001)

The enzymes that pass DNA through DNA so as to remove entanglements, adenosine-triphosphate-hydrolyzing type-II topoisomerases, are able to suppress the probability of self-entanglements (knots) and mutual entanglements (links) between ~10 kb plasmids, well below the levels expected, given the assumption that the topoisomerases pass DNA segments at random by thermal motion. This implies that a 10-nm type-II topoisomerase can somehow sense the topology of a large DNA. We previously introduced a ''kinetic proofreading'' model which supposes the enzyme to require two successive collisions in order to allow exchange of DNA segments, and we showed how it could quantitatively explain the reduction in knotting and linking complexity. Here we show how the same model quantitatively explains the reduced variance of the double-helix linking number (supercoiling) distribution observed experimentally.

DOI: 10.1103/PhysRevE.63.031909 PACS number(s): 87.14.Gg, 82.70.−y, 68.15.+e, 02.40.−k

I. INTRODUCTION

In many biological processes, chemical reactions between specific molecules (e.g., specific amino acids in the case of construction of proteins) must be tightly regulated and sequenced with low rates of error. At the molecular level regulation depends on the binding of biomolecules to particular targets. Hopfield [1] and independently, Ninio [2] considered the problem of explaining how many biological processes achieve error rates below those expected on the basis of the free-energy differences between ''correctly'' and ''incorrectly'' matched reactants.

Recognizing that all such cases used external sources of energy [e.g., in the form of adenosine triphosphate (ATP), which can be hydrolyzed to liberate $10k_BT$ of free energy], Hopfield and Ninio showed how by *repeating* a reversible recognition step one could reduce the probability of an incorrect match of reactants below that expected on thermodynamic grounds. For this reduction of the error rate to be achieved, the repeated recognition steps need to be separated by irreversible processes. Hopfield called such mechanisms ''kinetic proofreading'' reactions [1]. Both Hopfield [1] and Ninio [2] imagined them as applied to primarily energetic (enthalpic) interactions, where differing *off rates* would provide the main means of distinguishing correctly from incorrectly matched reactants.

In this paper we apply ideas similar to those of Ninio and Hopfield to a model for the mechanism of DNA topoisomerases, the enzymes that catalyze topology changes of DNA molecules in cells [3]. Recent experiments of Rybenkov *et al.* [4] showed that certain ATP-hydrolyzing topoisomerases are able to suppress the probability of knots, supercoils, and links of large DNA molecules, far below the level expected in thermodynamic equilibrium. To do this, the topoisomerases must sense the differences in *on rates*, i.e., differing rates of collision between DNA segments, between entangled and disentangled states. Here we show that a kinetic proofreading model, previously introduced [5] to describe suppression of knotting, also can explain the supercoiling suppression experiments. This model is based on a two-step process that provides more sensitivity to the differences in collision rates between entangled and disentangled DNA molecules than is possible in thermal equilibrium.

A. Topoisomerases catalyze passages of DNA through DNA

For simplicity, we shall only consider topoisomerases interacting with circular double-stranded DNA molecules, which have well-defined topologies. The topology of circular DNA can be changed in two distinct fashions. First, we can imagine changing the ''internal'' linking number Lk of the double helix itself [Fig. 1(a)]. Second, we can imagine passing one double-helix segment through another so as to knot a single circular DNA, or to link two (or more) circles [Figs.

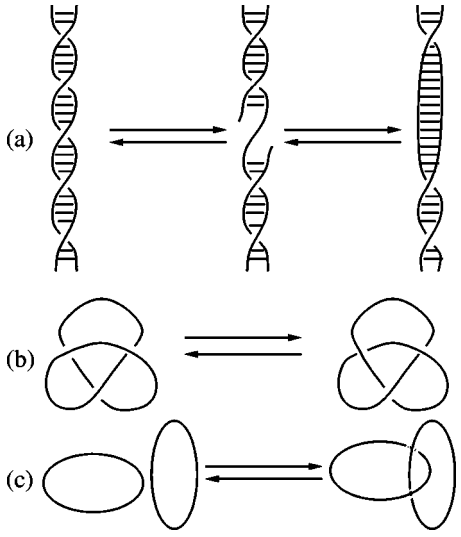

FIG. 1. Topology changes of circular DNA molecules. (a) Internal linking number of a double helix can be changed by temporarily breaking one of the sugar-phosphate backbones along a double-stranded DNA. (b) Knotting of a circular double-helix DNA can be changed by passing the double helix through itself. (c) Catenation (linkage) of two DNA molecules can be changed by passing one double helix through another.

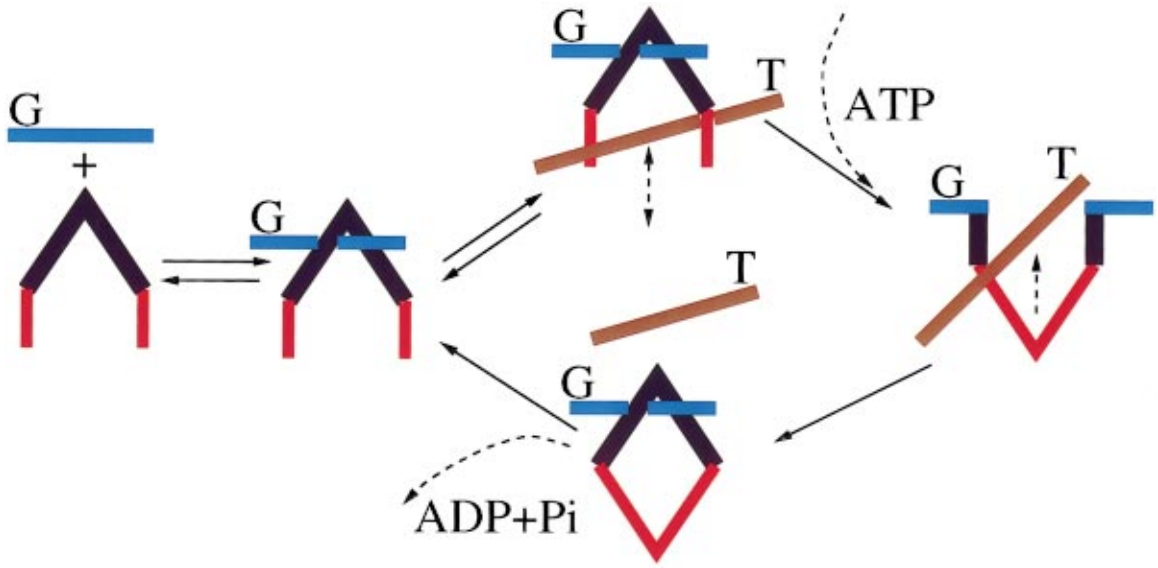

FIG. 2. (Color) Two-gate model of type-II topoisomerase function. The topoisomerase reversibly binds to a *G* (''gate'') segment. A bound *G* segment can then be reversibly cleaved by the enzyme. A second *T* (''transported'') segment can then fluctuate in and out of the gate. ATP binding irreversibly triggers enzyme conformational change which traps the *T* segment; the *T* segment is eventually transported out the other side of the enzyme. Finally, the products of ATP hydrolysis are released to reset the enzyme to its initial state.

1(b,c)]. Note that interlinking between two circular DNA molecules is often called *catenation* to distinguish it from the internal linking of the two strands in the DNA double helix.

There are two separate families of enzymes in all cells that are specialized to accomplish these two jobs. Type-I topoisomerases transiently cut *one* of the double-helix backbones to allow changes in internal duplex linking number. Type-II topoisomerases pass one double-helix segment through another, to allow changes in knotting of one molecule, or interlinking of double helices.

Most type-I topoisomerases are simple catalysts and act in thermal equilibrium; they thus allow internal linking number (and usually twisting stress) in a DNA to relax to its thermodynamic equilibrium value. If a type-I topoisomerase is allowed to equilibrate with circular DNA molecules in solution, a thermal distribution [6] of double helix linking numbers will eventually be obtained [7].

Most type-II topoisomerases hydrolyze ATP, thus releasing stored energy, during their reaction cycle of passage of double helix through double helix [8]. When first binding to DNA, they cut the molecule to form a double-helix-protein ''gate'' through which a second double-helical DNA segment can pass. The segment that is cut is called the *G* segment, while the segment that is transported through the gate is called the *T* segment. This transport process is unidirectional, and requires ATP binding to occur [8]. The enzyme normally binds two ATPs, hydrolyzing both of them during its reaction cycle [8–10], but the details of how ATP binding and hydrolysis are coupled to enzyme function are incompletely understood.

Experiments to date support a ''clamp'' model of how ATP binding and hydrolysis are coupled to the enzyme's mechanical function (Fig. 2) [11,12]. Supposing that a *G* segment is already bound, in the absence of bound ATP, the enzyme is in an ''open clamp'' state, allowing the *T* segment to freely enter and exit the gate entrance. ATP binding causes the clamp to close, and if there is a *T* segment caught in the clamp, it will be transported through the gap in the *G* segment to pass out through the exit on the opposite side of the enzyme. ATP hydrolysis occurs during this step. After release of the product of ATP hydrolysis, the enzyme returns to the open-clamp form, still bound to the *G* segment. At this point, the enzyme–*G*-segment complex has completed an entire DNA-passage cycle, and may either repeat (with a different *T* segment), or, following ligation of the cut in the *G* segment, the enzyme may dissociate from the *G* segment. The essential point is that ATP binding may be considered to be an irreversible step, triggering enzyme conformational change and eventual ATP hydrolysis.

In fact, ATP hydrolysis is not actually required for *G*-segment cleavage or religation: experiments on nonhydrolyzable ATP analogs show that the reaction proceeds all the way to *T*-segment passage [11]. Instead, ATP hydrolysis and product release appear necessary only for the final resetting of the enzyme to its initial state, i.e., reopening of the clamp and repair of the broken *G* segment.

While all type-II topoisomerases have this basic function, they can be divided into two subfamilies based upon details of their biological functions and differences in DNA interaction. Enzymes in one subfamily primarily decatenate interlinked DNA, and include all eukaryotic type-II topoisomerases as well as bacterial topoisomerase IV and phage *T*4 topoisomerase II. This family of DNA disentangling type-II topoisomerases is the focus of this paper. The second subfamily is comprised of bacterial gyrases that use ATP to negatively supercoil (i.e., unwind) DNA. Gyrases clearly utilize the energy released during ATP hydrolysis to apply internal torsional stress to DNA, increasing its free energy.

On the other hand, how the energy liberated by ATP hydrolysis is used by enzymes in the first subfamily is not

clear. The basic two-gate model described above does not describe how the DNA is affected by the irreversibility of the one-way strand transfer process. In fact, before 1997 the question of whether type-II topoisomerase incubated with DNA and ATP would generate a thermal distribution of knot, catenation or supercoil topoisomers was unanswered.

B. Experiments on topological simplification by type-II topoisomerases

In 1997, Rybenkov and co-workers [4] definitively established that in fact type-II topoisomers use ATP hydrolysis to strongly suppress knotting, catenation, and supercoiling of DNA molecules in solution to levels far below those expected from thermal fluctuation of topology. Thermal distributions of topoisomerase have long been studied, and may be prepared by the use of enzymes that change topology in thermal equilibrium (i.e., without ATP hydrolysis or other irreversible steps) such as topoisomerase I. Equilibrium distributions of knots and catenanes are usually generated by using DNA molecules that which have breaks or ''nicks'' along their sugar-phosphate backbones, which allow them to intermittently open in thermal equilibrium. After equilibration these nicks can be sealed up and the resulting topological distribution of the circular DNA molecules can then be analyzed.

For double-stranded DNA, the thermal knotting probability, given some equilibrium pathway to topology change, is well characterized experimentally and theoretically, and for a few kb DNA molecules, the probability of having a nontrivial knot is a few percent, with almost all the knots simple trefoils. This small knotting probability expresses the large entropic cost of constraining a few kb DNA to cross itself in a particular fashion. Rybenkov *et al.* [4] found that the probability of knotting of 10 kb $P4$ DNA is reduced from its equilibrium value of $P_{\mathrm{knot}}^{\mathrm{eq}}=0.031$, to only $P_{\mathrm{knot}}^{\mathrm{topo\ II}}=0.000\,62$ when a type-II topoisomerase and ATP were present. Likewise, the knotting probability for 7 kb $PAB4$ DNA was reduced from $P_{\mathrm{knot}}^{\mathrm{eq}}=0.017$ to $P_{\mathrm{knot}}^{\mathrm{topo\ II}}=0.0002$.

Similar experiments were done to examine DNA catenation; again, the comparison was for a DNA concentration where the probability of linkages occurring by thermal fluctuation of topology was a few percent. Although this type of experiment is somewhat more complicated than knotting, since it involves multiple molecules and therefore depends on the DNA solution concentration, the result was analogous to that for knotting. The probability for interlinkage of two 10-kb $P4$ DNA molecules was reduced from the equilibrium value $P_{\mathrm{linkage}}^{\mathrm{eq}}=0.064$ for certain concentration and solution conditions, to the much smaller $P_{\mathrm{linkage}}^{\mathrm{topo\ II}}=0.004$.

Rybenkov *et al.* also examined fluctuation of internal double-helix linkage number [Fig. 1(a)], or supercoiling of circular DNA molecules, comparing thermal equilibration via topoisomerase I, with the steady state obtained using topoisomerase II and ATP. The change in linking number from the value energetically preferred by an undistorted double helix (i.e., one turn per 10.5 bp), or $\Delta\mathrm{Lk}$ is the relevant quantity to consider, since $\langle\Delta\mathrm{Lk}\rangle_{\mathrm{eq}}=0$.

It is crucial to note that type-II topoisomerase is able to change double helix linking number, but only by steps of ± 2. This can be best illustrated by taking a thin paper strip and noting that the linkage number of its edges is changed by ± 2 when the strip is passed through itself. Rybenkov *et al.* found that the variance of the linking number distribution was reduced from its equilibrium value $\langle\Delta\mathrm{Lk}\rangle_{\mathrm{eq}}^{2}=3.1$ to the experimental value $\langle\Delta\mathrm{Lk}\rangle_{\mathrm{topo\ II}}^{2}=1.7$, for bacterial topoisomer IV.

C. Kinetic proofreading model and plan of this paper

In each of the three cases of knotting, catenation, and supercoiling, Rybenkov *et al.* thus demonstrated that topoisomerase II reduced the topological complexity below what would be expected for thermal fluctuation of topology, i.e., by Brownian segmental motion and collision [4]. Somehow, type-II topoisomerases recognize DNA molecules with complex topology and preferentially make strand passages on those molecules. This is only possible because type-II topoisomerases are machines (or motors) that use an external source of energy, i.e., ATP, to give them an irreversible cycle (Fig. 2). However, given ATP hydrolysis, it is not clear how the small (10 nm diameter) enzyme determines the topological state of a $>$ 1000 nm length of DNA.

The purpose of this paper is to show how a model we previously proposed [5] to explain the knot and catenation data can also simply explain the result for the reduction of supercoiling fluctuations. This model was based on the realization that the experimental results corresponded closely to the topological distributions in the presence of topoisomerases II being on the order of the *squares* of the distributions obtained thermally. We further realized that the enzyme could use its irreversible cycle to be sensitive to the *collision rate* of DNA segments, and that this information could plausibly provide the guidance necessary to reduce the topological complexity to the observed levels. The minimal model required to do this is one where two successive DNA-DNA collisions must occur within a short time window to achieve DNA strand passage. We call this general type of model a kinetic proofreading model, in reference to related models for molecular recognition processes [1,2].

In the remainder of the paper, we first briefly review our model for reduction of knot and catenation complexity in Sec. II. The discussion is particularly simple for these cases because for the few kb DNA molecules of interest, experimentally, transitions between only two topological states [unknot $\leftrightarrow$ trefoil knot, and unlink $\leftrightarrow$ single link, as in Figs. 1(b,c)] need be considered. By contrast, for the case of supercoiling, ''ladders'' of topological states must be treated, with transitions driven between states with Lk's differing by ± 2.

In Sec. III we review established results for thermal fluctuation of Lk, and for the free-energy cost of perturbing Lk from the relaxed (lowest free energy) state where there is one link per 10.4 bp of DNA. In Sec. IV we discuss how the free-energy differences between different supercoils can be used to estimate the rates of collisions that lead to transitions between the different states. This prepares us to present the

two-collision kinetic proofreading model applied to the case of supercoiling fluctuations in Sec. V. This section includes a quantitative comparison of the model and the experimental data.

We finally note that while we were preparing this paper, Zhang *et al.* [13] discussed a similar application of our kinetic proofreading model to supercoiling topoisomerasease. The results of their analytical work are rather similar to ours. They also present some kinetic data from simulations that support some of the assumptions we have made about the connection between collision rates and the free energy of topoisomers. These points will be discussed in Sec. V.

II. KINETIC PROOFREADING MODEL OF TYPE-II TOPOISOMERASES

The results of Rybenkov *et al.* [4] suggested to us that the apparent *squaring* of the probability distribution of topological states might be the result of a similar kinetic proofreading mechanism, but applied instead to the differing *on rates*, or *topology-dependent collision rates* that are the kinetic origin of the thermodynamic equilibrium distribution of topoisomerasease. Thus, we arrived at a two-collision model of type-II topoisomerases [5], which could be rather simply applied to the knotting and catenation experiments of Rybenkov *et al.* [4], since for the <10 kb DNA molecules studied, in equilibrium, the only appreciably likely topological states were a trivial state (unknot or unlink) and a nontrivial state (trefoil knot or single link).

We review the two-collision model for knot-unknot transitions (Fig. 3). Starting from either knots or unknots with a topoisomerase bound to a *G* segment (Fig. 3, state 1), a ''synapse'' between the *G* and a second *T* segment can reversibly occur (Fig. 3, $1\leftrightarrow 2$; this corresponds to the reversible *G*-*T* collision step of Fig. 2). For these states, note that the numbers ''1'' and ''2'' indicate how many DNA segments are bound by the topoisomerase. A key point is that polymer-conformational fluctuations drive the forward and reverse transitions at this step. Since the *T* segment must ''find'' the bound topoisomerase by random fluctuation, and since the polymer dynamics of the polymer will certainly depend on whether it is knotted or not, the on rate will depend on the topological state.

The off rate will depend only on the dynamics of a few statistical segments of polymer near the synapse, and perhaps on local interactions between the topoisomerase and the *T* segment. Both of these effects are going to be independent of topology so long as the knots are not so small that there is an elastic distortion of the DNA that can strongly affect its dynamics from the synapse state. Since we are considering >5 kb DNA molecules, and since a statistical segment is 300 bp, we are not in the elastic regime. We thus assume that the on rates (for knots κ, and for unknots υ) depend on topology but that the off rates (λ for both knots and unknots) do not.

If these collisions were allowed to pass DNA through DNA, they would generate topological changes. Under the assumption that all the collisions lead to topology change, the steady state would satisfy $\upsilon P^{\rm eq}_{\rm unknot}=\kappa P^{\rm eq}_{\rm knot}$. Here, $P^{\rm eq}_{\rm knot}$ and $P^{\rm eq}_{\rm unknot}$ are the equilibrium probabilities for the ''phantom'' case where DNA segments are permitted to freely pass through one another. With the additional assumption that the topoisomerase bound to DNA does not strongly influence its global conformation or its intermolecular collision rates, we then obtain $\upsilon/\kappa \approx P^{\rm eq}_{\rm knot}/P^{\rm eq}_{\rm unknot}$.

This identification is shown as approximate since collisions that do not change topology will also contribute to υ and κ. However, it is reasonable that the total self-collision rates differ strongly for few kb knots and unknots. Preliminary results from our own molecular dynamics simulations of knots and unknots verify this hypothesis, and will be published separately.

The next step in our model takes place from the synapse state 2. We suppose that an irreversible process can occur from 2, to a state 1* with the topoisomerase in an ''activated state'' (denoted by *), and with only one DNA segment bound (denoted by the 1). We imagine this to occur by a conformational change of the enzyme, combined with release of the *T* segment captured in the previous step. Irreversibility could be enforced via ATP binding, possibly coupled to topoisomerase conformation change and cleavage of the bound DNA. As no overall DNA conformational change is involved in this step, the rate α of this step is insensitive to DNA topology. The function of this step is to provide the irreversible step separating two recognition steps; for a second recognition step to occur, the first *T* segment must be released. The first collision ($1\leftrightarrow 2$) is used as a ''first pass'' of recognition, after which the topoisomerase is put into the activated ''*'' state which is able to effect an DNA strand passage.

The state 1* can irreversibly ''decay'' back to 1 at a topology-independent rate γ, giving spontaneous ''deactivation'' of the topoisomerase with no change in DNA topology. This decay process includes hydrolysis and release of the bound ATP, and enzyme conformational change back to the original state. However, before this decay can occur, a new synapse might reversibly form between a new DNA segment and the activated topoisomerase-DNA complex ($1^*\leftrightarrow 2^*$), that will lead to strand transfer. As before, the off-rates λ' are assumed insensitive to DNA knotting. As we are only concerned with topology-changing events, we may assume $\upsilon'/\kappa' \approx P^{\rm eq}_{\rm knot}/P^{\rm eq}_{\rm unknot}$.

If a recollision does occur, then irreversible transitions from $2^*\rightarrow 1$ achieve strand passage, DNA religation, and release of the passed segment. At the end of the $2^*\rightarrow 1$ transitions, the topoisomerase is reset and ready for another cycle. ATP hydrolysis and product release could be involved in this step. This irreversible transition should be controlled by local topoisomerase-DNA interactions, and should occur at a rate μ that is independent of DNA topology.

The chemical rate equations can easily be solved for their steady state, since all the reactions are unimolecular and the rate equations therefore linear. The steady-state knot/unknot ratio takes a simple form due to the symmetry between most of the rates on the knot and unknot sides of the reaction:

$$\frac{P_{\rm knot}}{P_{\rm unknot}}=\frac{(\gamma[\lambda'+\mu]+\kappa'\mu)}{(\gamma[\lambda'+\mu]+\upsilon'\mu)}\,\frac{\upsilon\upsilon'}{\kappa\kappa'}. \tag{1}$$

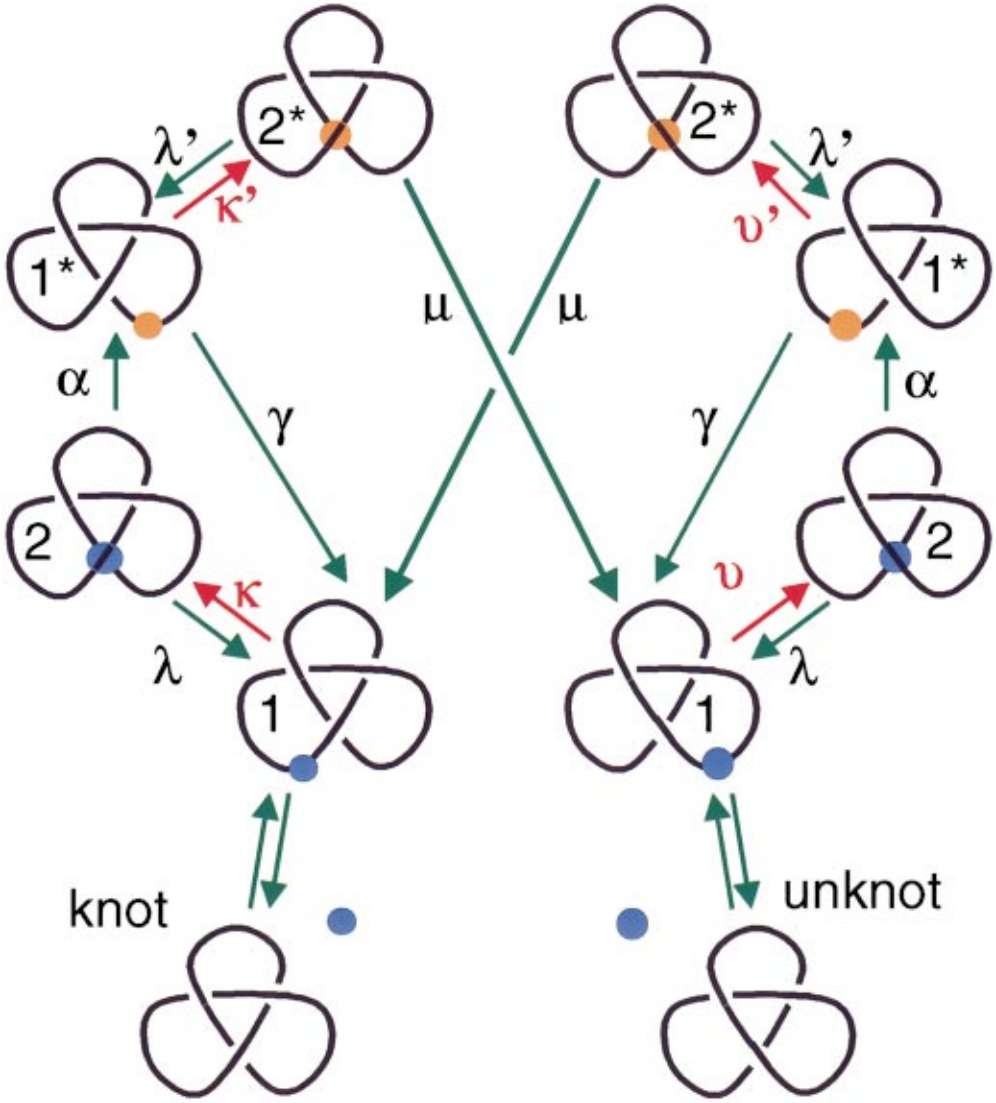

FIG. 3. (Color) Two-collision model for type-II topoisomerase that accomplishes kinetic proofreading of DNA topology. Self-collision or ''synapsing'' occurs twice along knotting and unknotting pathways. The labels ''1'' and ''2'' indicate the number of DNA segments bound to the topoisomerase; * indicates states where the topoisomerase is ''activated'' to be able to pass DNA through DNA (see text). The topoisomerase itself is shown in blue when inactive and red when active. By cascading two synapsis events separated by irreversible transitions, the first synapsis ($1\leftrightarrow 2$) delivers an excess of knots over unknots to the second synapsis ($1^*\leftrightarrow 2^*$); the second reaction thus ''proofreads'' the first. Proofreading can reduce the knot-to-unknot ratio to below $(P^{\mathrm{eq}}_{\mathrm{knot}}/P^{\mathrm{eq}}_{\mathrm{unknot}})^2$. Most of the transitions do not depend on knottedness (green arrows); all discrimination of topology is based on synapse formation rates (red arrows). The many topology-independent rate constants (e.g., dependent on DNA enzyme unbinding kinetics, which will be energetically and locally determined) do not contribute to the final knot-to-unknot steady-state ratio of this model.

The value of the decay rate γ plays a crucial role in Eq. (1). If $\gamma\rightarrow 0$, or the activation of the enzyme is permanent, and therefore always eventually leads to a strand transfer, then the steady-state knot/unknot ratio becomes υ'/κ', which we argued above to be just the equilibrium ratio. This occurs because without the decay pathway active, the two-step process simply delays the eventual approach to the thermodynamical equilibrium ratio. Put another way, in this limit, the topoisomerase has no internal time reference against which to measure the difference between collision rates on a DNA, and therefore will make random strand passages and will arrive at the thermodynamical knot/unknot distribution.

On the other hand, if γ is large enough so that $\gamma[\lambda'+\mu]\gg\kappa'\mu$ (and therefore also, so that $\gamma[\lambda'+\mu]\gg\upsilon'\mu$), then the decay pathway more rapidly depletes unknots than knots arriving at 1*, and there occurs a reduction of the knot/unknot ratio to

$$\frac{P_{\mathrm{knot}}}{P_{\mathrm{unknot}}}=\frac{\upsilon\upsilon'}{\kappa\kappa'}. \tag{2}$$

Thus, assuming that the ratio of the total self-collision rates υ/κ is roughly equal to that for the topology-changing rate ratio υ'/κ', we find that the reaction of Fig. 3 can re-

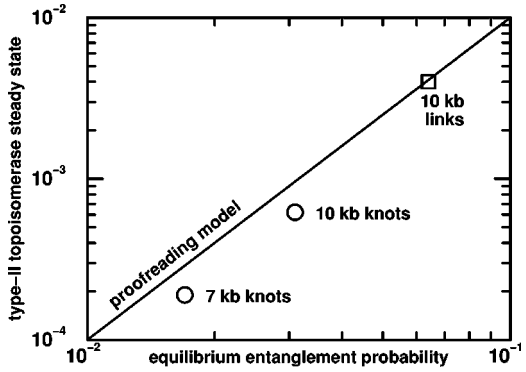

FIG. 4. Experimental knotting and linking probabilities of (symbols). Horizontal axis shows thermal equilibrium entanglement probability; vertical axis shows the steady-state result in presence of type-II topoisomerases and ATP. The kinetic proofreading model of the text is able to reduce knotting probability to levels below the line, which corresponds to *(steady state)=(equilibrium)*^{2}.

duce the ratio of the knot and unknot probabilities to the level of the *square* of $P^{\rm eq}_{\rm knot}/P^{\rm eq}_{\rm unknot}$. This was the main result of our previous paper [5]. In the $\gamma\rightarrow 0$ limit, all the topology-independent rate constants drop out of the final knot probability, leaving a result with no adjustable parameters, that represents the *optimal* reduction of knot and link complexity possible by this proofreading reaction.

Linking-unlinking of circular DNA molecules can be discussed in exactly the same way as the knotting-unknotting steady state discussed above, for the dilute solution conditions of Ref. [4]. In all the experiments, the unknot/unlink probabilities were nearly 1, with the knot/link probabilities at the level of a few percent, allowing the use of a two-state kinetic model. The two-step proofreading process, if optimized, could be expected to reduce the probability of knots and links in those experiments to a level as low as the *square* of the probabilities expected in thermodynamic equilibrium, i.e., to the $\approx 10^{-4}$ level.

The ''squared law'' derived above agrees well with the experimental results of Rybenkov *et al.* [4] for knotting and linking probabilities for DNA molecules incubated with type-II topoisomerases and ATP (Fig. 4). In our previous paper [5] we noted that the same model could also explain analogous results obtained by Rybenkov *et al.* [4] for supercoiling topoisomers, and that this provided additional support for our hypothesis that the type-II topoisomerases use a two-collision process.

In the next sections we discuss the thermodynamical distribution of supercoiling topoisomers, the kinetic rates that can be expected for collisions that interconvert those topoisomerasease, and the generalization of the model discussed in this section to the case of supercoiling topoisomers.

III. THERMAL EQUILIBRIUM LINKING NUMBER DISTRIBUTION

Thermal fluctuations of linking number Lk of a circular double-helix DNA are well characterized both experimentally [6,7] and theoretically [14–16]. The minimum free energy state has $\mathrm{Lk}=\mathrm{Lk}_0$, where Lk_0 is the DNA length in base pairs, divided by about 10.4, reflecting the energetically favored rate of winding of one strand around the other in the relaxed double helix. The free energy cost of supercoiling is essentially harmonic:

$$\frac{F(\mathrm{Lk})}{k_BT}=\frac{G}{2}(\mathrm{Lk}-\mathrm{Lk}_0)^2=\frac{G}{2}(\Delta\mathrm{Lk})^2. \tag{3}$$

There are some deviations from this harmonic behavior when $F\gg k_BT$, but since we are primarily interested in the thermal fluctuation regime $F\approx k_BT$, Eq. (3) is simple and accurate. In the experiments of Rybenkov *et al.* [4], the initial state for all type-II topoisomerase supercoiling experiments was this thermal distribution.

The stiffness G is numerically a bit less than that which would be assumed from a thermal fluctuation argument applied to DNA twisting, or $4\pi^2$ times the torsional stiffness of DNA in k_BT units (i.e., the twist persistence length $C\approx 100$ nm ≈ 300 bp), divided by the total DNA length L. The reduction of G below this value occurs because of *writhing*, or chiral bending, of the DNA backbone [16]. The scaling with L is expected so that the free energy is intensive (note that Lk is extensive). For DNA under physiological solution conditions, the stiffness observed experimentally is about $G\approx(2200\ \mathrm{bp})/L=(750\ \mathrm{nm})/L$ [16].

If Lk is allowed to thermally fluctuate, it will equilibrate to a Boltzmann distribution:

$$P^{eq}_{\rm Lk}\propto e^{-F(\mathrm{Lk})/k_BT}, \tag{4}$$

which leads to a Gaussian distribution:

$$P^{eq}_{\rm Lk}\propto\exp\left[-\frac{G}{2}(\Delta\mathrm{Lk})^2\right]. \tag{5}$$

The thermal fluctuations have amplitude $\langle(\Delta\mathrm{Lk})^2\rangle_{\rm eq}=1/G\approx L/2.2$ kb; the scaling follows from independent twisting and writhing fluctuations occurring in persistence-length regions along the molecule [16] For the 7 kb DNA studied by Rybenkov *et al.* [4], $G\approx 0.3$, and $\langle(\Delta\mathrm{Lk})^2\rangle_{\rm eq}\approx 3$.

IV. KINETICS OF Lk TRANSITIONS GENERATED BY TYPE-II TOPOISOMERASES

A. Odd- and even-Lk subpopulations are not mixed by type-II topoisomerases

Type-II topoisomerases can only change the linking number of circular DNA by ± 2. Therefore, after introducing topoisomerase II plus ATP into a solution of initially thermally equilibrated circular DNA molecules (assuming that the topoisomer II is the only available mechanism for topology change), Lk for any particular molecule will always be even or odd. The steady state distribution of Lk's obtained by the action of topoisomerase II is actually a sum of independent even-Lk and odd-Lk distributions.

The parity-conserving nature of type-II topoisomerase means that a molecule with linkage $\mathrm{Lk}=k$ can undergo only two transitions, $k\rightarrow k+2$ and $k\rightarrow k-2$. The kinetics of the

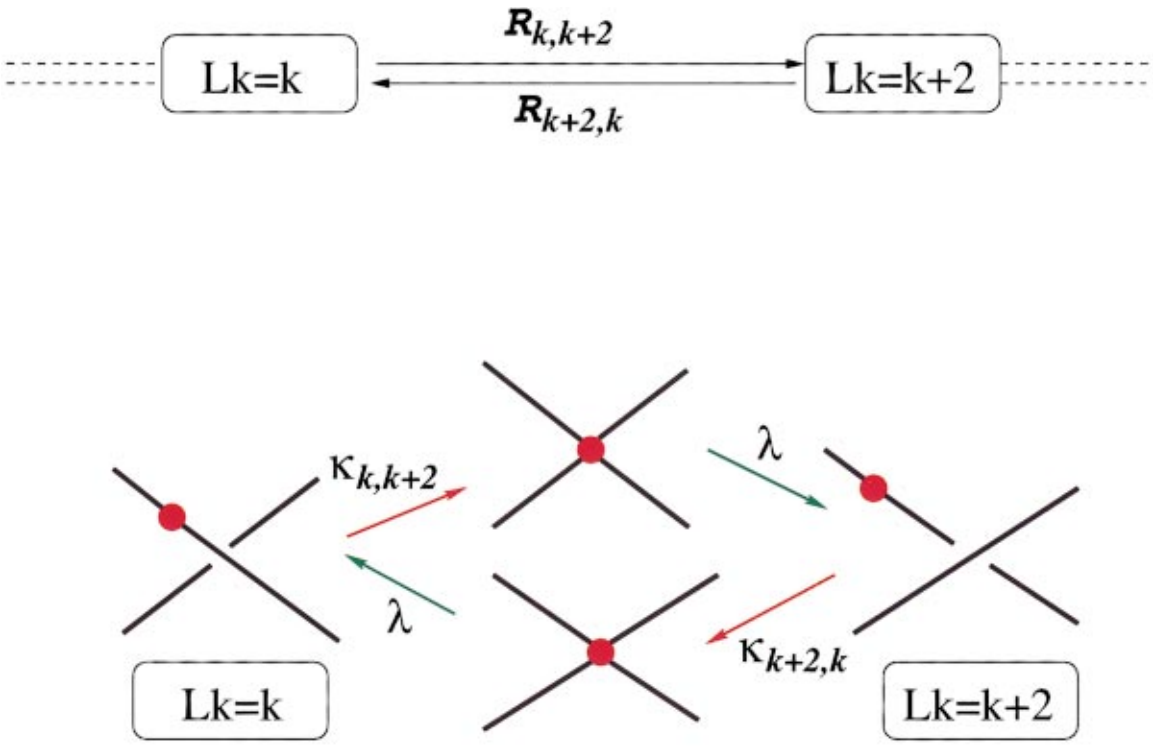

FIG. 5. (Color) Freely self-crossing passage reaction model of a type-II topoisomerase distinguishes two DNA-DNA ''synapse'' states. On isolated circular DNA molecules, transitions occur from Lk=k to Lk=$k+2$ at a rate $\kappa_{k,k+2}\lambda$, and back again at a rate $\kappa_{k+2,k}\lambda$. For a topoisomerase that does not consume stored energy, $\kappa_{k+2,k}/\kappa_{k,k+2}$ must be equal to the ratio of the thermal equilibrium probabilities of the states Lk=k and $k+2$.

combined topoisomerase-II–DNA system are therefore summarized by the transition rates $R_{k,k\pm2}$, for all integers k. The transitions thus are organized into two decoupled one-dimensional chains of reactions, for the odd- and even-Lk states (Fig. 5, top).

B. Detailed-balance-like condition for the steady state

The steady-state distribution attained by the type-II topoisomerase, P_{Lk}, satisfies

$$R_{k,k+2}P_k = R_{k+2,k}P_{k+2} \tag{6}$$

for all integers k, since otherwise there would be a net flow of probability along the one-dimensional ladders of states (Fig. 5, top). Neighboring states in each ladder therefore satisfy a ''detailed balance''-like condition in the steady state:

$$\frac{P_{k+2}}{P_k} = \frac{R_{k,k+2}}{R_{k+2,k}}. \tag{7}$$

This type of relation in general does not hold in nonequilibrium systems, but is forced here by the one-dimensional nature of the transitions of Lk.

C. Random-collision model

The simplest kinetic model for topoisomerase II activity is the ''random-collision'' or ''freely-self-crossing'' model, where the topoisomerase passes the T segment with some fixed probability after it hits the enzyme–G-segment complex. By construction, this model must reach thermal equilibrium for the even- and odd-Lk groups of molecules, since all that is being introduced is a reversible and unbiased transition path between states with different Lk. Another way to see that thermal equilibrium must be reached by this model is to realize that its statics must be identical to those of a ''phantom'' polymer that is allowed to occasionally freely pass through itself.

If the topology distribution is initially thermally equilibrated, then introduction of a topoisomerase II that makes strand passages after random collision will therefore not change the Lk distribution. Since this was the manner in which the experiments of Rybenkov *et al.* [4] were carried out, topoisomerase II was not carrying out strand passages following simple random collisions. However, it will be useful for the discussion of the kinetic proofreading model to analyze the random-collision model in slightly more detail.

The $k\rightarrow k+2$ and $k+2\rightarrow k$ transitions (Fig. 5, top) can be decomposed into collision (''on'') steps that form a ''synapse'' between the T and G segments, and exit (''off'') steps leading away from the synapses. We label the on rates as $\kappa_{k,k+2}$ and $\kappa_{k+2,k}$. These transition rates will depend on k since the rate at which collisions leading to particular topology changes will obviously depend on details of the proximity of DNA segments to one another, which depends on the degree of supercoiling.

On the other hand, the kinetics of segments exiting a synapse are essentially independent of k. This is because a seg-

ment exits at a rate determined by its interaction with the enzyme (e.g., its local unbinding kinetics) and by its fluctuation dynamics on the scale of a fraction of a DNA persistence length, which are k independent. Thus we label all the synapse exit process with a single off rate λ, giving rates $R_{k,k+2}=\kappa_{k,k+2}\lambda$ and $R_{k+2,k}=\kappa_{k+2,k}\lambda$.

Since the steady state of this model is the thermal equilibrium of the odd- and even-Lk populations, the ratio of the κ's is thus constrained:

$$\frac{P_{k+2}}{P_k}=\frac{P_{k+2}^{\mathrm{eq}}}{P_k^{\mathrm{eq}}}=\frac{\kappa_{k,k+2}}{\kappa_{k+2,k}} \tag{8}$$

for every integer k. This identification of the on rates with properties of the equilibrium distribution will be an important tool in the next section. Note that $P_{\mathrm{Lk}}\neq P_{\mathrm{Lk}}^{\mathrm{eq}}$ since the steady-state distribution has separate even- and odd-Lk normalizations; the total numbers of even- and odd-Lk molecules cannot be changed by type-II topoisomerases.

D. A simple model for the on rates

We will need a bit more information about the on rates $\kappa_{k,k\pm2}$ in order to completely compute the probability distribution resulting from our proofreading model. The main feature that we want the dynamics to exhibit is a tendency for the collision rates to go up with $\Delta\mathrm{Lk}$, since as the molecule is made more supercoiled, it will writhe, and therefore self-collide more frequently. Perhaps the simplest kinetic model that does this and is consistent with Eq. (8) are simple thermally activated kinetics:

$$\kappa_{k,k\pm2}=re^{F(k)/k_BT}. \tag{9}$$

This model has rates that satisfy Eq. (8) and are therefore consistent with thermal equilibration of the freely-crossing model; that increase with the free energy of the initial state ($\mathrm{Lk}=k$); and that do not depend on the final state ($\mathrm{Lk}=k\pm2$). This independence on the final state means that in state k, transitions occur with equal probability to the two adjacent states. This will be very nearly true in the random-coil fluctuation regime relevant to the experiments, where the linkage numbers are less than or equal to the total number of persistence lengths along the molecule.

The common factor r is proportional to the characteristic collision rate of one site on a molecule with other sites along that molecule times a factor associated with segment capture by the topoisomerasease. The characteristic rate r will be very roughly the DNA segment orientational relaxation rate $k_BT/(\eta b^3)\approx10^5\ \mathrm{sec}^{-1}$ since the collisions experienced by a segment in a long polymer are mainly with adjacent segments along the molecule. The rate r will not actually appear in our final results because we need only ratios of rates such as Eq. (9) with nearby values of k.

V. KINETIC PROOFREADING MODEL APPLIED TO SUPERCOILING

Our double-collision model for type-II topoisomerases [5] can be placed into each step of the chain of Lk transitions (Fig. 6). In comparison to the random collision model of Fig. 5, the double collision proofreading model contains irreversible steps and reaction cycles. As was the case for knots and links, this model is a kind of machine that can supress supercoiling complexity. The transition rates between $\mathrm{Lk}=k$ and $\mathrm{Lk}=k+2$, $R_{k,k+2}$ and $R_{k+2,k}$ are different from those in the random-collision model. Steady states established for the odd- and even-Lk distributions that differ from the thermal distributions. However, Eq. (7) still holds for the steady-state distribution:

$$\frac{P_{k+2}}{P_k}=\frac{R_{k,k+2}}{R_{k+2,k}}. \tag{10}$$

The rates $R_{k,k+2}$ and $R_{k+2,k}$ are determined by the reaction of Fig. 6, bottom. The analysis carried out previously [5] (Sec. I) gives

$$\frac{R_{k,k+2}}{R_{k+2,k}}=\frac{(\gamma[\lambda'+\mu]+\mu\kappa_{k+2,k})}{(\gamma[\lambda'+\mu]+\mu\kappa_{k,k+2})}\frac{\sigma_k}{\sigma_{k+2}}\frac{\kappa_{k,k+2}}{\kappa_{k+2,k}}. \tag{11}$$

As before, the only topologically dependent transition rates are the σ and κ collision, or on rates. The rate σ_k is the *total* rate of all possible collisions. We have already seen that collisions are of two types, based on our analysis of the random-collision model (Sec. III), corresponding to the pathways for Lk changing by ±2. Thus $\sigma_k=\kappa_{k,k+2}+\kappa_{k,k-2}$.

As for the application of our model to removal of knots and links, we assume a large enough decay rate γ so that $\gamma[\lambda'+\mu]\gg\kappa'\mu$ and $\gamma[\lambda'+\mu]\gg\nu'\mu$. This limit leads to

$$\frac{R_{k,k+2}}{R_{k+2,k}}=\frac{\sigma_k}{\sigma_{k+2}}\frac{\kappa_{k,k+2}}{\kappa_{k+2,k}}=\left(\frac{\kappa_{k,k+2}+\kappa_{k,k-2}}{\kappa_{k+2,k}+\kappa_{k+2,k+4}}\right)\frac{\kappa_{k,k+2}}{\kappa_{k+2,k}} \tag{12}$$

in exact analogy to our previous results for the effectively two-state knotting and linking problems [5].

The topology-dependent rates υ, υ', κ, and κ' are determined by thermal fluctuations. Note that in contrast to the knotting and catenation problems, all collisions correspond to a topology-changing pathway for Lk. Thus, since we are considering the $\gamma\to\infty$ limit, we may assume the primed and unprimed rates to be essentially the same.

Equation (8) connects the topology-changing collision rate-ratio to the *thermal equilibrium* distributions:

$$\frac{\kappa_{k,k+2}}{\kappa_{k+2,k}}=\frac{P_{k+2}^{\mathrm{eq}}}{P_k^{\mathrm{eq}}}. \tag{13}$$

Therefore,

$$\begin{aligned}\frac{P_{k+2}}{P_k}&=\left(\frac{\kappa_{k,k+2}}{\kappa_{k+2,k}}\right)^2\frac{1+(\kappa_{k,k-2}/\kappa_{k,k+2})}{1+(\kappa_{k+2,k+4}/\kappa_{k+2,k})}\\&=\left(\frac{P_{k+2}^{\mathrm{eq}}}{P_k^{\mathrm{eq}}}\right)^2\frac{1+(\kappa_{k,k-2}/\kappa_{k,k+2})}{1+(\kappa_{k+2,k+4}/\kappa_{k+2,k})}.\end{aligned} \tag{14}$$

The steady-state odd- and even-Lk distributions are driven away from the equilibrium distributions to be the square of

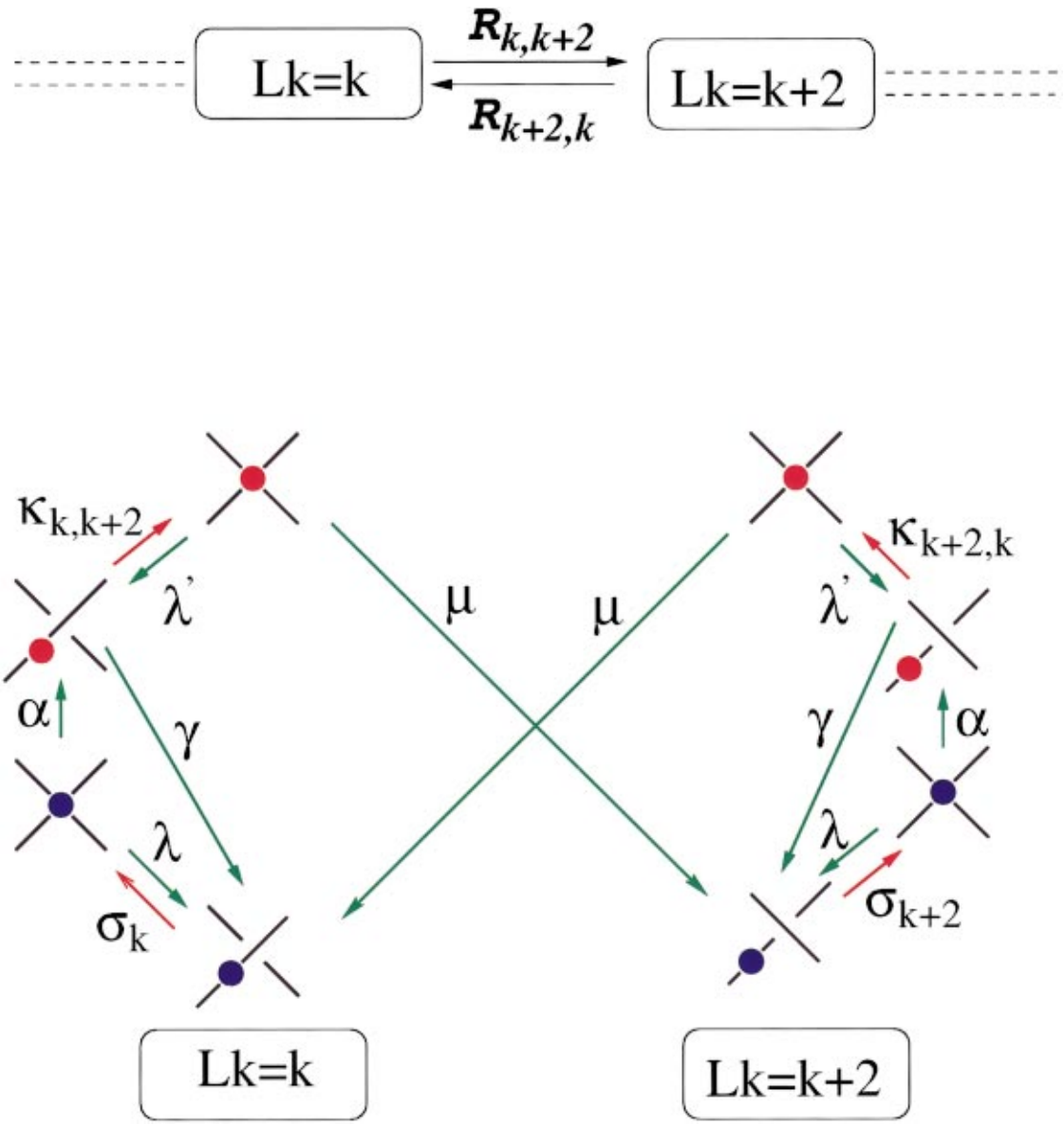

FIG. 6. (Color) Double collision model for type-II topoisomerase. Top: transitions occur from Lk=k to Lk=$k+2$ at a net rate $R_{k,k+2}$, and back again at a rate $R_{k+2,k}$. Bottom: the net transition rates follow from the double collision model applied between the states Lk and Lk+2. For a large activated state decay rate γ, $R_{k,k+2}/R_{k+2,k}=(\sigma_k/\sigma_{k+2})(\kappa_{k,k+2}/\kappa_{k+2,k})\approx(\kappa_{k,k+2}/\kappa_{k+2,k})^2$ (see text).

the equilibrium distribution times a correction factor. Since $\kappa_{k,l}$ is l independent the remaining rate ratios are just $\kappa_{k,k-2}/\kappa_{k,k+2}=1$ and $\kappa_{k+2,k+4}/\kappa_{k+2,k}=1$, giving simply

$$\frac{P_{k+2}}{P_k}=\left(\frac{P_{k+2}^{\mathrm{eq}}}{P_k^{\mathrm{eq}}}\right)^2. \tag{15}$$

Thus, the steady-state shape of the Lk distributions will still be nearly Gaussian, but with half the variance of the equilibrium distribution, roughly what was observed experimentally [4]. The squaring of the whole distribution is in exact analogy to the squaring of the knot-to-unknot and unlink-to-link ratios discussed previously [5].

Finally, given the ratio of the number of odd-Lk molecules to the even-Lk molecules $N_{\mathrm{odd}}/N_{\mathrm{even}}$, we can write the steady-state distribution for the odd-Lk molecules:

$$P_k=\frac{A}{1+N_{\mathrm{even}}/N_{\mathrm{odd}}}(P_k^{\mathrm{eq}})^2, \tag{16}$$

and for the even-Lk ones:

$$P_k=\frac{A}{1+N_{\mathrm{odd}}/N_{\mathrm{even}}}(P_k^{\mathrm{eq}})^2, \tag{17}$$

up to an overall constant A determined by the normalization condition $\Sigma P_k=1$. If a type-II topoisomerase experiment is

started from a thermally equilibrated sample (as done in Ref. [4]), one will have $N_{\rm even} \approx N_{\rm odd}$ for few kb DNA molecules.

A. Comparison with experiment

We now use the results (16) and (17) to compare the distribution predicted by our model with the experimental results for 7-kb DNA molecules [4]. Lk_0 is the molecule length divided by the helix repeat of 10.4 bp, or $\mathrm{Lk}_0 = 673$. The experimentally observed thermal fluctuation of linking number is $\langle \Delta \mathrm{Lk} \rangle_{\rm eq}^2 = 1/G = 3.1$. Thus the equilibrium distribution is Gaussian, with a width of $\Delta \mathrm{Lk} = 1.7$.

To compute the distribution generated by our kinetic proofreading model we need to know the fractions of molecules present initially with even and odd Lk, i.e., $N_{\rm even}/N$ and $N_{\rm odd}/N$, where $N = N_{\rm even} + N_{\rm odd}$. This follows from the fact that the experimenters thermally equilibrated the supercoiling of their sample before adding type-II topos and ATP. Thus from (5) we know

$$\frac{N_{\rm even}}{N_{\rm odd}} = \frac{\sum_{k=0,\pm 2,\pm 4,\ldots} P_{\rm Lk}^{\rm eq}}{\sum_{k=\pm 1,\pm 3,\pm 5,\ldots} P_{\rm Lk}^{\rm eq}}. \tag{18}$$

For the parameters relevant to the experiments [4] this ratio is $N_{\rm even}/N_{\rm odd} = 1.000\,001$, very nearly unity.

The result of the proofreading model for the experimental case is therefore very close to the square of the equilibrium distribution, i.e., $P_k = A(P_k^{\rm eq})^2$ where A is the normalization. Thus the width of the proofreading steady-state distribution is half the width of the thermal distribution. To see how close this is to the experimental data, we present our distribution in the form of Fig. 2 of Ref. [4]. Instead of plotting the distribution, those authors plotted

$$-\frac{\ln(P_{\rm Lk})/\ln(P_{\rm Lk_0})}{\mathrm{Lk}-\mathrm{Lk}_0}. \tag{19}$$

For the equilibrium distribution (5) with $\langle (\Delta \mathrm{Lk})^2 \rangle = 3.1$ this should plot as a line through the origin with slope $G/2 \approx 0.16$; the experimental results can be seen to follow this law (Fig. 7, stars).

The proofreading model predicts a steady-state distribution that is Gaussian with half the width of the equilibrium distribution, i.e., $\langle (\Delta \mathrm{Lk})^2 \rangle = 1.55$, which plots as a straight line with slope 0.32 in Fig. 7 (diamonds). This can be seen to be just slightly steeper than the experimental data for the steady-state distribution [4] obtained using a type-II topoisomer (*E. coli* topoisomerase IV, Fig. 7, crosses). The experimental data fit to a line of slope 0.29, corresponding to a variance $\langle (\Delta \mathrm{Lk})^2 \rangle = 1.7$.

Rybenkov *et al.* also published the reduction of the variances of $\langle (\Delta \mathrm{Lk})^2 \rangle$ obtained using a number of type-II topoisomeraseases, relative to the equilibrium variance $\langle (\Delta \mathrm{Lk})_{\rm eq}^2 \rangle$. For *E. coli* topoisomerase IV, the variance was reduced by a factor $3.1/1.7 = 1.8$, which is slightly below the ratio 2.0 predicted by the model of this paper. Other topoisomerases gave reductions in variances from 1.35 to 1.7 times. This suggests that type-II topoisomerases may be ''leaky,'' perhaps by occasionally becoming ''activated'' by thermal conformational fluctuation of the enzyme. Some level of ''errors'' in the operation of the machine of Fig. 6, and some variation of this error rate from enzyme to enzyme, is a plausible explanation for the variation in the variance reduction observed experimentally.

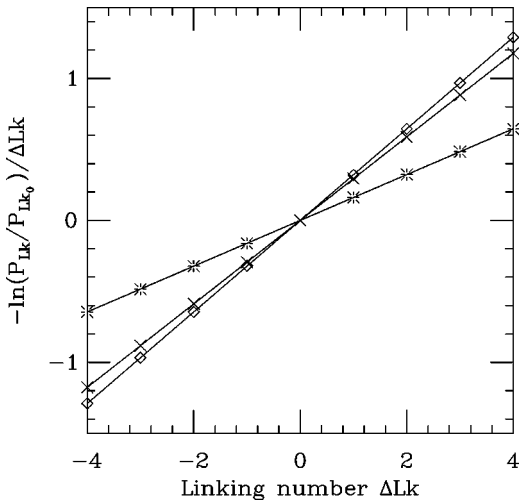

FIG. 7. Comparison of the linking number distributions obtained in thermal equilibrium (stars), in the type-II topoisomerase-driven steady state of Ref. [1] (crosses), and from the two-collision kinetic proofreading model of the present paper (diamonds). What is plotted is the logarithm of the probability distribution divided by $\Delta \mathrm{Lk}$, and therefore a Gaussian distribution will yield a straight line, with slope equal to $(2\langle \Delta \mathrm{Lk} \rangle^2)^{-1}$. The proofreading model and type-II topoisomerase distributions are in close agreement, each showing roughly double the slope of the equilibrium distribution.

One way to add such error pathways to the model is to permit additional transitions between the $\mathrm{Lk} = k$ and $k+2$ states of Fig. 6. These error pathways provide a transition between adjacent topoisomers of the same parity that is in parallel to the proofreading transition. If these error transitions are thermally activated, their rates must satisfy detailed balance. This is perhaps most easily seen if one imagines the ATP-hydrolyzing part of the reaction to be turned off: then the steady state will be achieved by the thermal error transitions alone, and must be the thermal equilibrium distribution. If the error rates are sufficiently large, the error transitions will drive the steady state to the equilibrium distribution.

B. Comparison with theory of Zhang *et al.*

While this paper was being prepared, Zhang *et al.* [13] made calculations similar to those presented here. Zhang *et al.* also used our two-step model [5] applied to the chain of transitions between different-Lk states. The main difference between the works appears to be the use of a Monte Carlo simulation of the dynamics of circular DNA to estimate the rates that we estimated analytically in Sec. III D.

While Zhang *et al.* did not present their results in precisely the form of Fig. 7, they also computed the probability distribution for the steady-state model using their Monte

Carlo calculation. They therefore had to assign numerical values to the rates of Fig. 6. They studied the steady-state probability distribution as a function of the decay rate γ for the activated state, and found that for sufficiently large γ, the steady-state value of $\langle(\Delta \mathrm{Lk})^2\rangle$ was driven below its thermal equilibrium value. They also noted that by tuning the value of γ the degree of reduction in variance of the Lk distribution could be tuned so as to fit data for the different enzymes studied experimentally [4].

Zhang *et al.* thus provided a valuable verification of the correctness of the assignment of the collision rates for molecules with different Lk we made in Sec. III D. More generally they have demonstrated via explicit computer simulation the feasibility of the basic topological proofreading concept discussed previously from an analytical perspective [5]. The main limitation of the simulations of Zhang *et al.* is the use of Monte Carlo dynamics to draw conclusions about relatively short-distance and short-time collision dynamics of DNA. It would be worth repeating their study using a more realistic molecular dynamics simulation, e.g., Brownian dynamics as developed by Vologodskii and co-workers for the study of DNA-site juxtapositions [17].

VI. CONCLUSION

We have described application of our two-collision model [5] for simplification of the topology of DNA molecules below equilibrium levels by type-II topoisomerases, to double-helix linking number Lk. Our model effectively senses the self-collision rates of molecules, using the information gained from the two collision steps — information that is *stored* in irreversible conformational change of the enzyme-DNA complex — to push the probability of knots, links, and supercoils below their equilibrium levels.

We have presented a straightforward generalization of our previous result of knotting and linking probabilities attained with topoisomerases being *squared* relative to the thermal equilibrium levels, namely, that the entire distribution of Lk becomes squared: $P_{\mathrm{Lk}}^{\mathrm{topo}} \propto (P_{\mathrm{Lk}}^{\mathrm{eq}})^2$. Since the equilibrium distribution is a nearly Gaussian distribution centered on Lk_0, the type-II topoisomer+ATP distribution is also essentially Gaussian, but with half the width, i.e., $\langle(\Delta \mathrm{Lk})^2\rangle_{\mathrm{topo}} = 0.5\langle(\Delta \mathrm{Lk})^2\rangle_{\mathrm{eq}}$.

The Gaussian shape of the steady-state distribution and its reduction in variance relative to the equilibrium distribution reproduce corresponding effects observed experimentally for a number of ATP-hydrolyzing type-II topoisomerases [4]. In addition our theoretical distribution is in quantitatively good agreement with the distribution obtained with *E. coli* topoisomerase IV, which is the most potent entanglement-removing type-II topoisomerase. Thus our basic two-collision model can explain diverse results for supression of knotting, linking, and now supercoiling.

Of course our model cannot be considered as ''proven'' until the chemical-mechanical cycle of a type-II topoisomerase is completely dissected. From a chemical standpoint, there has been recent progress in demonstrating that the two ATP hydrolysis steps occur at different times during the topoisomerase cycle [9,10]. Progress has also recently been made in studying the mechanical operation of a type-II topoisomerase directly, via micromanipulation of the DNA template [18]. These techniques may allow the question of whether or not two DNA-topoisomerase collisions precede strand transfer to be answered.

ACKNOWLEDGMENTS

We acknowledge helpful discussions with D. Chatenay, N.R. Cozzarelli, G.B. Mindlin, V. Rybenkov, E.D. Siggia, A.V. Vologodskii and E.L. Zechiedrich; J.F.M. and J.Y. acknowledge support of the NSF through Grant No. DMR-9734178, Research Corporation, the Petroleum Research Fund, the Whitaker Foundation, and the University of Illinois Foundation. M.O.M. acknowledges support of the Sloan Foundation and the Mathers Foundation.

[1] J.J. Hopfield, Proc. Natl. Acad. Sci. U.S.A. **71**, 4135 (1974).
[2] J. Ninio, Biochimie **57**, 587 (1975).
[3] J.C. Wang, J. Biol. Chem. **266**, 6659 (1991).
[4] V.V. Rybenkov, C. Ullsperger, A.V. Vologodskii, and N.R. Cozzarelli, Science **277**, 690 (1997).
[5] J. Yan, M.O. Magnasco, and J. Marko, Nature (London) **401**, 932 (1999).
[6] R. E. Depew and J. C. Wang, Proc. Natl. Acad. Sci. U.S.A. **72**, 4275 (1975).
[7] D. E. Pulleyblank, M. Shure, D. Tang, J. Vinograd, and H. P. Vosberg, Proc. Natl. Acad. Sci. U.S.A. **72**, 4280 (1975).
[8] J. C. Wang, Q. Rev. Biophys. **31**, 107 (1998); Annu. Rev. Biochem. **65**, 635 (1992).
[9] T.T. Harkins, and J.E. Lindsley, Biochemistry **37**, 7292 (1998); **37**, 7299 (1998).
[10] C.L. Baird, T.T. Harkins, S.K. Morris, and J.E. Lindsley, Proc. Natl. Acad. Sci. U.S.A. **96**, 13 685 (1999).
[11] J. Roca and J.C. Wang, Cell **77**, 609 (1994).
[12] J. Roca and J.C. Wang, Cell **71**, 833 (1992).
[13] Y. Zhang, H.J. Zhou and Z.-C. Ou-Yang (unpublished).
[14] K.V. Klenin, A.V. Vologodskii, V.V. Anmshelevich, A.M. Dykhne, and M.D. Frank-Kamenetskii, J. Mol. Biol. **217**, 413 (1991).
[15] A.V. Vologodskii, S.D. Levene, K.V. Klenin, M. Frank-Kamenetskii, and N.R. Cozzarelli, J. Mol. Biol. **227**, 1224 (1992).
[16] J.F. Marko and E.D. Siggia, Phys. Rev. E **52**, 2912 (1995).
[17] H. Jian, T. Schlick, and A. Vologodskii, J. Mol. Biol. **284**, 287 (1998).
[18] T.R. Strick, V. Croquette, and D. Bensimon, Nature (London) **404**, 901 (2000).